Journal of proteome research

Article

pubs.acs.org/jpr

Metabonomic Profiling of TASTPM Transgenic Alzheimer's Disease Mouse Model

Ze-Ping Hu,[†,§] Edward R. Browne,[‡] Tao Liu,[§] Thomas E Angel,[§] Paul C. Ho,[†] and Eric Chun Yong Chan*[,†]

[†]Department of Pharmacy, Faculty of Science, National University of Singapore, 18 Science Drive 4, Singapore 117543

[‡]GlaxoSmithKline R&D China, Singapore Research Centre, Biopolis at One-North, 11 Biopolis Way, The Helios #03-01/02, Singapore 138667

[§]Biological Sciences Division, Pacific Northwest National Laboratory, Richland, Washington 99352, United States

ABSTRACT: Identification of molecular mechanisms underlying early stage Alzheimer's disease (AD) is important for the development of new therapies against and diagnosis of AD. In this study, nontargeted metabonomics of TASTPM transgenic AD mice was performed. The metabolic profiles of both brain and plasma of TASTPM mice were characterized using gas chromatography−mass spectrometry and compared to those of wild-type C57BL/6J mice. TASTPM mice were metabolically distinct compared to wild-type mice (Q^2Y = 0.587 and 0.766 for PLS-DA models derived from brain and plasma, respectively). A number of metabolites were found to be perturbed in TASTPM mice in both brain (D-fructose, L-valine, L-serine, L-threonine, zymosterol) and plasma (D-glucose, D-galactose, linoleic acid, arachidonic acid, palmitic acid and D-gluconic acid). In addition, enzyme immunoassay confirmed that selected endogenous steroids were significantly perturbed in brain (androstenedione and 17-OH-progesterone) and plasma (cortisol and testosterone) of TASTPM mice. Ingenuity pathway analysis revealed that perturbations related to amino acid metabolism (brain), steroid biosynthesis (brain), linoleic acid metabolism (plasma) and energy metabolism (plasma) accounted for the differentiation of TASTPM and wild-type mice. Our results provided insights on the pathogenesis of APP-induced AD and reinforced the role of TASTPM in drug and biomarker development.

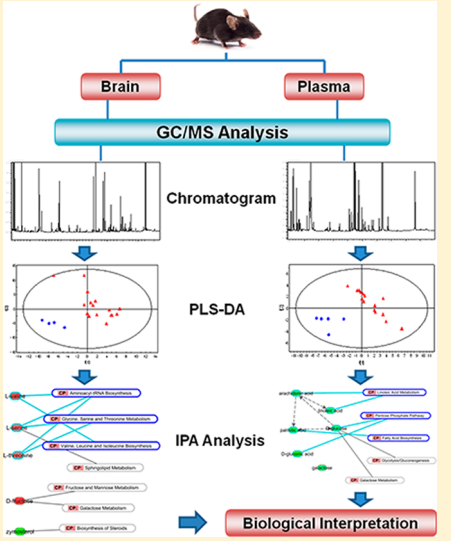

KEYWORDS: *Alzheimer's disease, metabonomics, metabolic profiling, biomarker, GC−MS, metabolic pathway, pathogenesis*

INTRODUCTION

Alzheimer's disease (AD) is a major cause of neurodegeneration and dementia. Identification of biomarkers associated with early stage AD is important for the development of new therapies and early diagnosis of the disease. However, accurate diagnosis of AD at the early stage of its pathogenesis remains difficult due to its complex spectrum of symptoms. Currently, the definitive diagnosis of AD is only possible post-mortem by detecting the two hallmark biomarkers, namely, the β-amyloid (Aβ) plaques derived from amyloid precursor protein (APP) and neurofibrillary tangle (NTF) derived from hyperphosphorylated tau protein, in the brain tissue of deceased patient.[1] Therefore, biomarkers derived from global profiling techniques performed on readily accessible biofluids, such as cerebrospinal fluid (CSF), plasma, serum and urine, are pertinent to elucidate the underlying metabotype of AD.

Genomics,[2,3] transcriptomics,[4,5] and proteomics[6,7] have been used extensively in the biomarker discovery of AD. It has been proposed that the integration of knowledge derived from these "-omic" studies will greatly advance our understanding of the development of AD, establish its early diagnosis, and ultimately help to improve and tailor the treatments.[8] Metabonomics, the global nontargeted profiling of endogenous metabolites, provides an alternative "-omic" approach to this array of "-omic" technologies.[9] Metabonomics plays an increasingly prominent role in biomarker identification of various neurodegenerative disorders,[10] such as Parkinson's disease,[11] Huntington disease,[12] schizophrenia,[13] and Batten disease.[14] Emerging metabonomics studies on AD patients and animal models are reported using mass spectrometry (MS), magnetic resonance spectroscopy (MRS) and nuclear magnetic resonance (NMR) spectroscopy (Table 1).[15−27] Most of these animal model-based studies utilized mice with genetic modifications on APP with or without presenilin (PS). Recent evidence suggests that systemic metabolite levels associate strongly with the development of AD than previously believed.[28,29]

Transgenic AD mouse models are essential for the understanding of disease pathophysiology, development of

Received: July 19, 2012
Published: October 19, 2012

Downloaded via TSINGHUA UNIV on October 23, 2021 at 09:25:31 (UTC).
See https://pubs.acs.org/sharingguidelines for options on how to legitimately share published articles.

 © 2012 American Chemical Society

Table 1. Reported Metabonomic-Based Biomarker Studies on AD

species	sample tested	analytical method	publishing year	refs #
APPTg2576 mice	brain	^{1}H MRS	2004	[15]
PS2APP mice	brain	^{1}H MRS	2005	[16]
APP-PS1 mice	brain	^{1}H MRS	2005	[17]
SAMP8 mice	serum	^{1}H NMR	2008	[18]
human	serum	^{1}H NMR	2008	[19]
human	plasma	UPLC−MS	2009	[20]
CRND8 mice	brain	^{1}H NMR	2010	[21]
human	plasma	UPLC−MS	2010	[22]
human	CSF	LC-ECA	2010	[23]
human	plasma	LC−MS	2011	[24]
APP/PS1 mice	brain	GC−MS	2012	[25]
human	plasma	LC−MS	2012	[26]
human	CSF	GC−MS and LC−MS/MS	2012	[27]

robust behavioral models and prediction of outcomes from potential therapies in drug development. Several novel transgenic AD mouse models, such as APPTg2576,[15] APP-PS2,[16] APP-PS1,[17] APP23,[30,31] APP[V7171],[32] and TASTPM,[33−37] have been developed focusing on the APP-processing and presenilin-1 (PS1) pathway as well as tau pathology. Each model has unique pathologies that provide insights into disease mechanisms and interactive features of neuropathologic cascades, which may potentially help in our understanding of the disease pathogenesis.[38] Several animal models of AD have been used in biomarker studies using metabolic profiling techniques.[15−18,21] TASTPM, heterozygote double mutant mice overexpressing both the 695-amino acid isoform of human APP (APP695) harboring the Swedish double familial AD mutation (K670N, M671L) and human PS1 harboring the familial mutation M146V were generated and maintained at GlaxoSmithKline.[34,37] Although the PS1 transgene alone does not cause amyloid plaque deposition,[39] the addition of mutant PS (a risk factor for familial AD) to create double transgenic models results in the acceleration of amyloid plaque deposition in APP mice.[40] In the TASTPM mouse model, expression of the two transgenes results in progressive amyloid deposition and pathology in the brain. Aβ (Aβ 1−40, Aβ 1−42 and total Aβ) loads increase with age between 3 and 6 months of age.[34] Meanwhile, TASTPM mice exhibit an age-dependent cognitive impairment in the object recognition test as compared to the wild-type animals, with the impairment becoming apparent from 6 months of age.[34] This double mutant transgenic line has been widely used in neuroscience studies.[33,36,41] However, the metabolic profiling of TASTPM mice has not been investigated thus far. In addition, no study has yet reported metabolite biomarkers in both brain and plasma in a transgenic AD animal model.

In this study, a gas chromatography−mass spectrometry-based (GC−MS-based) metabonomic technique was explored for the metabolic profiling of both brain and plasma samples to identify perturbations in biochemical pathways related to the TASTPM AD mouse model. In addition, enzyme immunoassay (EIA) was performed to monitor the perturbation of endogenous steroidal metabolites.

MATERIALS AND METHODS

Chemicals and Reagents

Methoxyamine hydrochloride and pyridine (ACS grade) were purchased from Sigma-Aldrich Chemical Co. (St. Louis, Mo. USA). The commercial derivatization reagent, MSTFA containing 1% TMCS was obtained from Pierce Biotechnology (Rockford, IL, USA). HPLC-grade methanol and acetonitrile were purchased from Tedia Company Inc. (Fairfield, OH, USA). HPLC grade toluene and acetone were from J.T. Baker (Mallinckrodt Baker, Phillipsburg, NJ, USA) and Mallinckrodt UltimAR (Mallinckrodt Baker), respectively. Water was Milli-Q grade purified by a Milli-Q UV purification system (Millipore, Bedford, MA, USA). All other chemicals and reagents used for the experiments were of analytical, HPLC or GC grade that were commercially available. The EIA kits for the determination of testosterone, androstenedione, dehydroepiandrosterone (DHEA), cortisol, estriol, and 17-hydroxy-progesterone were obtained from Diagnostic Systems Laboratories (Webster, TX, USA); kits for progesterone (PROG) and estradiol were from Cayman Chemical (Ann Arbor, MI, USA); and kit for corticosterone was from Assay Design (Ann Arbor, MI, USA).

Animals and Grouping Schedules

All studies were conducted in accordance with the GSK Policy on the Care, Welfare and Treatment of Laboratory Animals and were reviewed by the GSK Institutional Animal Care and Use Committee or by the ethical review group at the institution where the work was performed. Each animal was housed in an individual cage at controlled temperature (25 ± 1 °C) and humidity (55 ± 5%) and provided with 12-h light/dark cycle. Animals had free access to standard laboratory diet and water during the experiments. TASTPM (n = 16) and wild-type C57BL/6J (n = 5) male mice at the age of 50-week old were maintained at the specific pathogen free laboratory of GlaxoSmithKline (Harlow, UK).

Plasma Sample Preparation for Metabonomics

Plasma samples were collected from the TASTPM (n = 16) and wild-type (n = 5) mice. To collect the blood, each mouse was deeply anesthetized with 200 μL of ketamine/xylazine mixture (75 mg/kg, 5 mg/kg) by intraperitoneal (i.p.) injection. Blood was collected by cardiac puncture into an Eppendorf tube precoated with 20 μL of 5% ethylenediaminetetra acetic acid (EDTA) in Milli-Q water as anticoagulant. The syringe (1 mL) was coated with 5% EDTA to avoid coagulation during blood sampling. The collected blood was placed on ice for 30 min and centrifuged at 3000g for 15 min at 4 °C. The plasma was collected and transferred to individual Eppendorf tubes, snap-frozen in liquid nitrogen and stored at −80 °C until further processing.

The plasma sample was prepared according to the protocol reported previously[42] with minor modification. Briefly, 950 μL of methanol/water mixture (8:1 v/v) was added to 50 μL of plasma, vortex-mixed vigorously for 1 min, and incubated at −20 °C for 30 min. After being centrifuged at 16000g for 30 min at 4 °C, a 900 μL aliquot of the supernatant was then transferred to a deactivated glass tube with screw cap and evaporated to dryness under a stream of nitrogen using TurboVap LV evaporator. Then, 200 μL of toluene was added to each sample, vortex-mixed for 1 min, and evaporated under nitrogen to remove the trace amount of water residue. After that, 30 μL of methoxyamine hydrochloride in anhydrous pyridine (20 mg/mL) was added, and the solution was vortexed

dx.doi.org/10.1021/pr300666p | J. Proteome Res. 2012, 11, 5903−5913

vigorously for 10 min. Methoximation reaction was performed at 60 °C for 1 h and room temperature (23 ± 1 °C) for 16 h. Each sample was trimethylsilylated at 60 °C for 1 h by adding 70 μL of MSTFA with 1% TMCS as catalyst. Finally, each derivatized sample was combined with 50 μL of GC-grade hexane, vortex-mixed for 1 min, and transferred subsequently to a 300-μL glass conical insert for GC−MS analysis within 24 h.

Brain Sample Preparation for Metabonomics

For both TASTPM and wild-type mice, the whole brain (including cerebellum but excluding olfactory bulbs) was rapidly collected and stripped of meninges. After rinsing with ice-cold 1× phosphate buffered saline (PBS) buffer, each brain was cut longitudinally. The tissues were transferred to individual Eppendorf tubes, snap-frozen in liquid nitrogen and stored at −80 °C until further processing.

The right half of the brain (∼200−300 mg) was thawed at 4 °C, weighed and recorded. After adding 2 mL/g of tissue of Milli-Q water, brain tissues were homogenized thoroughly using a Heidolph DIAX 900 homogenizer (Heidolph Instruments, Germany). After each homogenization, the probe was washed with methanol/water (50/50, v/v) twice to avoid any crossover contamination. All the procedures were performed on ice. After vortex-mixing, a 100 μL aliquot of the brain homogenate was used for the metabonomic study.

Brain samples were prepared according to the protocol reported previously[43] with minor modification. Each brain homogenate (100 μL) aliquot was added with 1 mL of prechilled one-phasic mixture solvent of methanol/chloroform (2:1, v/v), vortex-mixed for 3 min, ultrasonicated in water bath for 10 min and incubated at −20 °C for 30 min. The sample was then centrifuged at 16000*g* and 4 °C for 30 min. A 900 μL aliquot of the supernatant was then transferred to a deactivated glass tube. The protein pellets were re-extracted using 1 mL of one-phasic mixture of chloroform/methanol/water (2:5:2, v/v/v), and the supernatant was collected and pooled with the previous extraction. The combined extract was evaporated to dryness under a stream of nitrogen using TurboVap LV evaporator. Then, 200 μL of toluene was added to each sample, and the mixture was vortex-mixed for 1 min and evaporated under nitrogen to remove the trace amount of water residue. Thereafter, dried residue of each sample was subjected to the same derivatization steps as described above.

Plasma and Brain Sample Preparation for EIA

Plasma samples were analyzed directly using EIA kits without further processing. Brain samples were homogenized as described above, and the volume of each homogenate was recorded and kept at −80 °C until analysis. To extract the steroids, the thawed brain homogenate was added with approximately 5 mL of methanol−acetic acid (99:1, v/v).[44] The homogenate was then ultrasonicated (Ultrasonik 57H; Ney Company, Bloomfield, USA) for 15 min, vortex-mixed for 1 min, and centrifuged at 6000*g* and 4 °C for 15 min. The supernatant was collected, while the precipitate was re-extracted twice with 5 mL of methanol−acetic acid (99/1, v/v) and centrifuged at 10000*g* and 4 °C for 15 min. The supernatants were combined and evaporated to remove the methanol under nitrogen at 50 °C using TurboVap LV. The remaining acetic acid mixture was subjected to freeze-drying (Labconco Corporation, Kansas City, Missouri, USA) at 0.14 mBar and −50 °C for 6 h. The dried residue was reconstituted with methanol−water (50/50, v/v) to the concentrations of 1 g of brain tissue/mL and stored at −80 °C prior to testing (this solution was subsequently referred to the brain extract). Aliquots of brain extract (0.5 mL, corresponding to 500 mg of brain tissue) were pipetted into a tube and diluted with 4 mL of Milli-Q water. The final organic content of methanol in the mixture was 5%. The samples were then applied to a preconditioned Strata-X SPE cartridge (200 mg adsorbent, 6 mL volume). The sulfated steroids were eluted with 4 mL of methanol−water (40/60, v/v), followed by unconjugated steroids being eluted with 4 mL of methanol. The organic solvent of the resultant unconjugated fractions was collected into a screw-cap deactivated glass tube (VWR Scientific) and evaporated under a gentle stream of nitrogen at 50 °C. The resultant residue was dissolved in 1 mL of assay buffer in the EIA kit package for analysis.

GC−MS Metabonomics

A Shimadzu QP-2010 GC−MS system (Shimadzu Corp., Japan) was used for the metabonomic experiments. A 30-m length DB-5 MS (5% phenyl polysilphenylene-siloxane phase) fused silica capillary column was used for separation (250 μm i.d., 0.25 μm film; J&W Scientific, Folsom, CA, Agilent Technologies, Palo Alto, CA, USA). For each sample, a fresh microvial was taken to avoid sample carryover and cross-contamination. The derivatized metabolites in the biological samples were injected in the split mode at a split ratio of 20:1. The injector temperature was set at 250 °C. Helium, the carrier gas, was maintained at a constant flow rate of 1 mL/min during the analysis. The column temperature was initially kept at 60 °C, where it was held for 1 min, and then ramped to 280 °C at 5 °C/min, where it was kept for 1 min, and further increased to 300 °C at 20 °C/min, where it remained for 5 min. The interface temperature and ion source were set at 250 and 200 °C, respectively. Electron impact (EI) ionization mode was used for mass detection, with an electron energy of 70 eV. Mass spectra were acquired with a scan range of m/z 50−700 and an acquisition rate of 20 spectra per second. Chromatogram acquisition, data handling, automated peak deconvolution and library search were performed using the GC−MS solution software (Version 2.5, Shimadzu Corp., Japan).

EIA of Endogenous Steroids

EIA was performed according to the manufacturer's instructions. The sensitivity and precision of each kit were examined in our laboratory and confirmed to be suitable for the analysis. To avoid interassay variation, all the samples were analyzed within one plate. In addition, the samples were stored in small aliquots to avoid potential degradation due to the repeated freeze−thaw cycles.

The absorbance was measured at 450 nm with reference 600 nm using Tecan Infinite 200 Microplate Reader (Tecan, Switzerland). The standard curves were fitted with four-parameter logistic data reduction, Sigmoidal model, using GraphPad Prism (La Jolla, CA, USA). The steroid concentrations were expressed as ng/mL or pg/mL of plasma, or ng/g or pg/g of brain tissue.

Data Preprocessing

The biological samples used for each metabonomic investigation were analyzed as a single batch and in a random order to minimize any systematic analytical error and subjective interference. In this way, retention time shift among the samples in one batch was kept to a minimum. Each sample analysis resulted in a GC−MS total ion current (TIC) chromatogram generated by GC−MS solution. These TIC

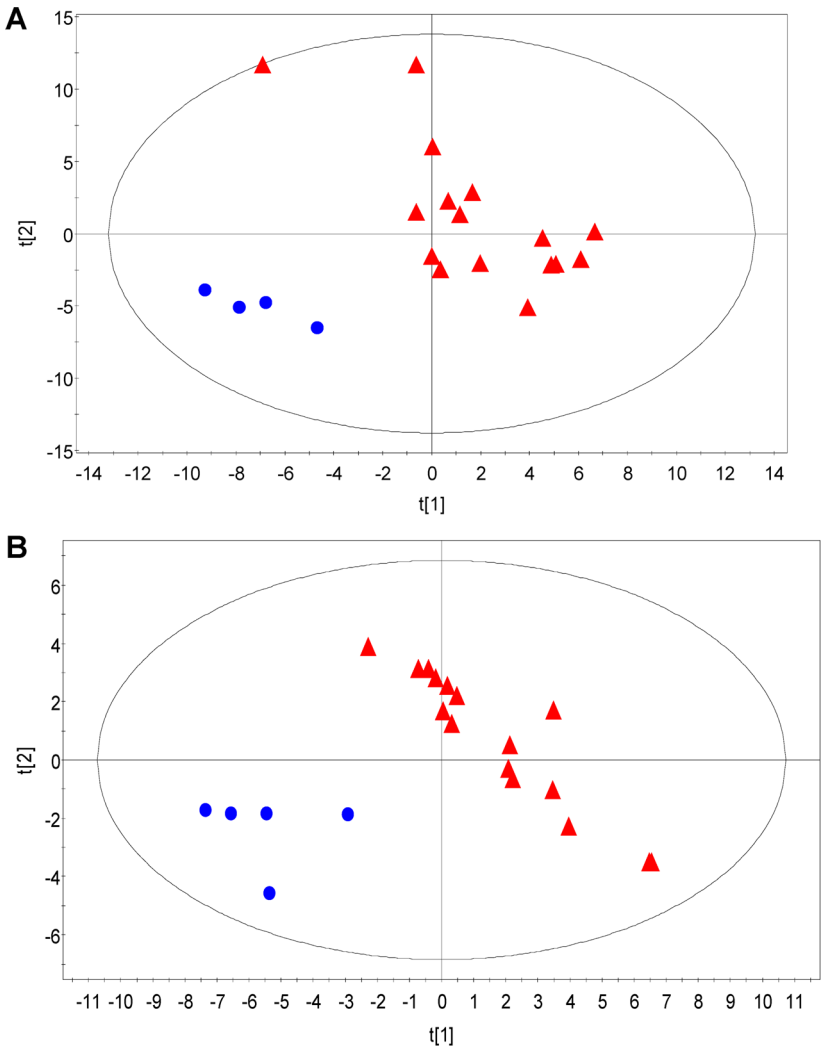

Figure 1. PLS-DA score plots of GC−MS variables detected in whole brain (A, R^2X = 0.444; R^2Y = 0.847; Q^2Y = 0.587; LV = 2) and plasma (B, R^2X = 0.339; R^2Y = 0.936; Q^2Y = 0.766; LV = 2) samples, separating TASTPM (50-week old, red triangle, n = 16) and wild-type C57BL/6J mice (50-week old, blue dot, n = 5, with one missing brain sample) groups.

chromatograms were evaluated and compared by observing the overlapped peaks to confirm the chromatographic reproducibility of the method. One chromatogram obtained from a TASTPM mouse sample was used to generate a mass chromatogram (MC) compound table. As only the intensity of the target ion was used for the peak integration, the peak area of MC was expected to be smaller than that derived from TIC where the intensities of all the fragmented ions were integrated. Therefore, MC was selected for the peak area integration due to its higher specificity.

In order to create a robust and interpretable model, the chromatographic peaks associated with each GC−MS profile were extracted as variables for each sample. The peaks with height signal-to-noise (S/N) values lower than 10 were rejected. Only peaks that were detected consistently in at least 80% of the TIC in each specific group were included. Those metabolites due to column bleed and derivatization reagent or showed no biological significance were excluded. The mass spectra obtained were inspected manually and searched rigorously using the National Institute of Standards and Technology (NIST) 05 (2005) and NIST05s libraries with EI spectra. Only those variables with matching similarity index (SI) greater than 70% were assigned putative metabolite identities. Some metabolites were identified by comparison to mass spectra and retention times of an in-house reference mass spectra database that were acquired with authentic standard compounds under identical data acquisition parameters (D-fructose, L-valine, L-serine, D-glucose, palmitic acid, and arachidonic acid). The identified metabolites were further searched using HMDB (Human Metabolome Database) and KEGG (Kyoto Encyclopedia of Genes and Genomes). Within each sample, the peak area for each detected peak was normalized against the sum of the total integral peak area within that sample chromatogram. Normalized area values were used as variables for the subsequent multivariate data analysis.

Multivariate and Univariate Data Analyses

All multivariate analyses and modeling on the normalized data were carried out using SIMCA-P 12.0 (Umetrics, Umeå, Sweden). The preprocessed data sets were mean-centered and unit-variance scaled before being subjected to principal component analysis (PCA) to visualize the clustering trend. Brain and plasma samples of both TASTPM and wild-type mice were further subjected to partial least squares discriminant analysis (PLS-DA) for the screening of discriminant metabolites that characterized the metabotypes. Metabolites with

dx.doi.org/10.1021/pr300666p | J. Proteome Res. 2012, 11, 5903−5913

variable importance in the projection (VIP) values of greater than 1 were regarded as potential marker metabolites. For this group of metabolites, independent unpaired Welch's t test was further performed using SPSS 16.0 (SPSS, Inc., Chicago, IL, USA) to test for statistical significance (p-value of less than 0.05).

For EIA of steroids, differences between two groups were analyzed using unpaired t test with unequal variances assumed. The criterion for statistical significance was set as $p < 0.05$.

Ingenuity Pathway Analysis (IPA)

To evaluate the metabolic perturbations associated with TASTPM mouse model, metabolic pathway analysis (IPA, www.ingenuity.com) was performed on the significantly perturbed metabolites determined by Wilcoxon rank sum test. IPA characterized the pathways and functions associated with the marker metabolites and AD as manifested in TASTPM mice. The metabolites were also cross-searched using HMDB (Human Metabolome Database) and KEGG (Kyoto Encyclopedia of Genes and Genomes).

RESULTS

Multivariate and Univariate Data Analysis

Brain and plasma samples obtained from TASTPM (50-week old, $n = 16$) and wild-type C57BL/6J (50-week old, $n = 5$) mice were investigated. The GC−MS TIC chromatograms of TASTPM mice yielded 143 and 75 chromatographic peaks detected in brain and plasma, respectively. The PCA scores plots displayed classification trends between the TASTPM and C57BL/6J mice, with all the observations falling within the Hotelling T^2 (0.95) ellipse (brain: $R^2X = 0.595$; $Q^2Y = 0.26$; PCs = 3; and plasma: $R^2X = 0.637$; $Q^2Y = 0.0267$; PCs = 5). Subsequently, supervised PLS-DA demonstrated distinct classification of TASTPM and C57BL/6J mice along the first latent variable (LV) (Figure 1). The statistics parameters confirmed that the PLS-DA models discriminated between TASTPM and C57BL/6J mice with regards to both brain ($R^2X = 0.444$; $R^2Y = 0.847$; $Q^2Y = 0.587$; LV = 2) and plasma ($R^2X = 0.339$; $R^2Y = 0.936$; $Q^2Y = 0.766$; LV = 2) matrices. The PLS-DA models were also validated and passed the permutation tests. The dominant marker metabolites influencing the differentiation between TASTPM and C57BL/6J mice were identified and listed in Table 2.

The results showed that a number of metabolites were significantly perturbed in TASTPM mice in both brain and plasma when compared to the wild-type mice. In brain, the levels of D-fructose, L-valine, L-serine and L-threonine were found to be higher, while zymosterol was lower in TASTPM mice. In plasma, none of the metabolites significantly changed in the brain were also found to be dysregulated herein. In addition, no identified metabolite was found to be elevated, while D-glucose, D-galactose, linoleic acid, arachidonic acid (AA), palmitic acid and gluconic acid were decreased in TASTPM mice when compared to the wild-type animals.

Characterization of Metabolic Pathways

The metabolic networks for the significantly perturbed metabolites in brain (D-fructose, L-valine, L-serine, L-threonine, and zymosterol) were significantly correlated with specific metabolic pathways of amino-acyl-tRNA biosynthesis (L-valine, L-serine and L-threonine), glycine, serine and theronine metabolism (L-serine and L-threonine) and valine, leucine and isoleucine biosynthesis (L-valine) (Figure 2). In plasma, the perturbed metabolites (D-glucose, D-galactose, linoleic acid, AA, palmitic acid, and gluconic acid) were significantly correlated with metabolic pathways of linoleic acid metabolism (linoleic acid and AA), pentose phosphate pathway (D-glucose and gluconic acid), and fatty acid biosynthesis (palmitic acid) (Figure 3). In addition, some other metabolic pathways associated with TASTPM were found to be correlated marginally with the perturbed metabolites in brain (sphingolipid metabolism, fructose and mannose metabolism, galactose metabolism, and biosynthesis of steroids) and plasma (glycolysis/gluconeogenesis and galactose metabolism) (Figures 2 and 3).

Table 2. Marker Metabolites Identified from Brain and Plasma Samples of TASTPM (50-week old, $n = 16$) and Wild Type C57BL/6J Mice (5-month old, $n = 5$, with one missing brain sample)

metabolite	sample	VIP	p^a	fold change[b]	SI[c]
D-fructose[d]	brain	1.94	<0.0001	1.71	73
L-valine[d]	brain	1.84	<0.001	1.45	87
L-serine[d]	brain	1.89	<0.001	1.25	81
L-threonine[d]	brain	1.81	<0.05	1.17	91
zymosterol	brain	1.83	<0.01	−1.16	75
D-glucose[d]	plasma	1.03	<0.05	−1.10	87
D-galactose	plasma	1.01	<0.05	−1.15	89
linoleic acid	plasma	1.16	<0.001	−1.18	93
AA	plasma	1.49	<0.05	−1.30	91
palmitic acid[d]	plasma	1.05	<0.01	−1.26	92
gluconic acid	plasma	1.63	<0.05	−2.06	88

[a]P-value calculated using Welch's t test. [b]Fold changes when TASTPM was compared to wild-type group. [c]SI (%) of library search. [d]Identity was confirmed using authentic standards.

EIA of Endogenous Steroids

The concentrations of steroids in C57BL/6J and TASTPM mice are presented in Figure 4. In TASTPM mice, the brain androstenedione level was dramatically decreased ($p < 0.05$) in brain. Notably, 17-OH-progesterone was not detectable in TASTPM brain, while it was readily detected in that of control animals (Figure 4A). In plasma, both cortisol and testosterone were significantly decreased in TASTPM than in C57BL/6J mice (Figure 4B). No significant difference was observed between these two groups for the other tested steroids, although corticosterone was marginally decreased in brain, while androstenedione, estradiol and PROG were lower in levels in plasma.

DISCUSSION

Brain

The elevated amino acids (serine, threonine and valine) found within the brain of TASTPM mice corroborated with a study showing that the hippocampal levels of several amino acids, including alanine, glycine, lysine and serine, were significantly increased in the APP/PS1 mouse model when compared to nontransgenic littermates.[25] Interestingly, the fold changes of the amino acids in the hippocampal brain[25] were consistently higher than those in the whole brain as revealed in this study. This might indicate that the metabolic perturbation induced by the AD could be region-specific in the brain. A clinical study also found that the plasma levels of several amino acids were significantly changed in patients with early stage AD when compared to that of the control subjects.[45] L-Serine is a key

dx.doi.org/10.1021/pr300666p | J. Proteome Res. 2012, 11, 5903−5913

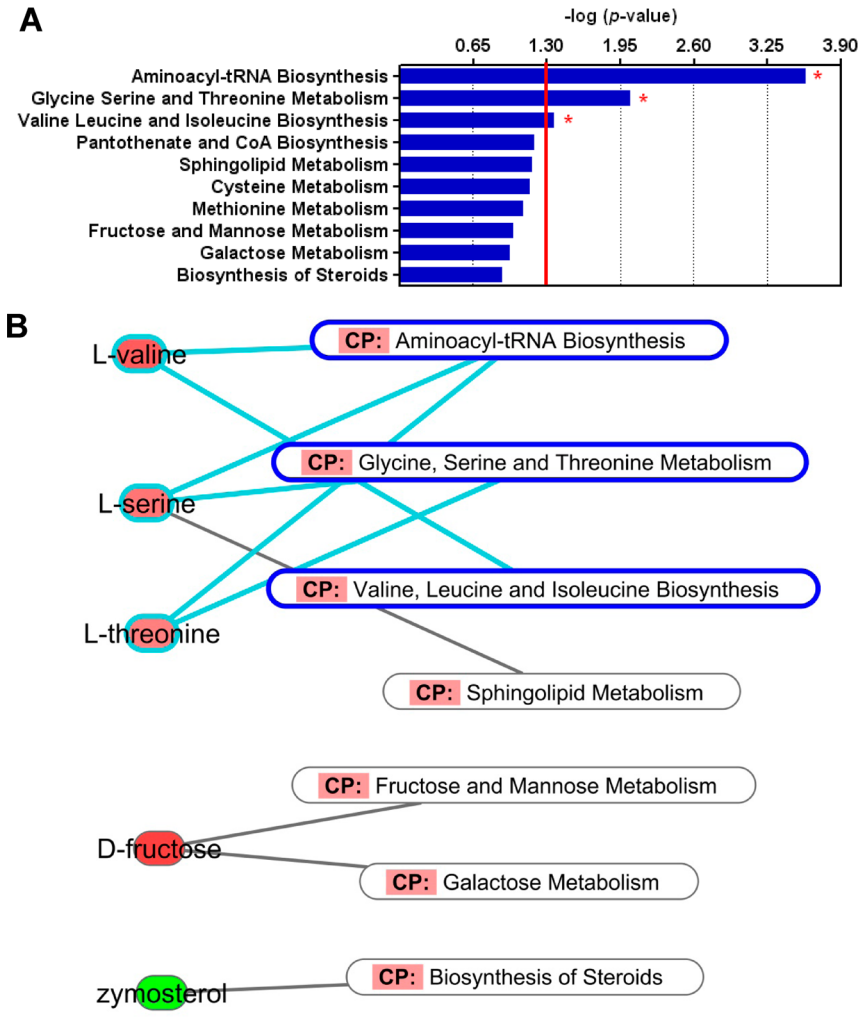

Figure 2. IPA of the significantly changed metabolites in the brain samples of TASTPM mice when compared to wild-type mice. (A) Metabolic canonical pathways (CPs) significantly associated with the perturbed metabolites in TASTPM mice as indicated by the $-\log p > 1.30$ (equivalent to $p < 0.05$). The figure was regenerated on the basis of the data exported from the IPA analysis using GraphPad for high-resolution purpose. (B) IPA provided significant inter-relations among these perturbed metabolites (increased as indicated in red, while decreased as indicated in green) and the metabolic CPs (highlighted in blue box) in TASTPM mice. The marginally perturbed metabolic CPs were not highlighted in the blue box.

metabolite in the pathway of sphingolipid metabolism. Studies of brain tissue samples from human and animal models suggested that perturbed sphingomyelin metabolism is a pivotal event in the dysfunction and degeneration of neurons that occurs in AD dementia.[46−49] In addition, D-serine, which can be synthesized from L-serine by the biosynthetic enzyme serine racemase in the mammalian brain, is an intrinsic coagonist of the *N*-methyl-D-aspartate (NMDA) glutamate receptor. NMDA receptors are key excitatory neurotransmitter receptors in the brain,[50] which mediate some extent of calcium-mediated neurotoxicity exerted by the Aβ.[51] D-Serine binds with high affinity to a coagonist site at the NMDA receptors and, along with glutamate, mediates several important physiological and pathological processes, including NMDA receptor transmission, synaptic plasticity and neurotoxicity.[52] It has been reported that the selective degradation of D-serine with D-amino acid oxidase greatly attenuated NMDA receptor-mediated neurotransmission, while the inhibitory effects of the enzyme were fully reversed by exogenously applied D-serine.[53] Another study showed that the serum levels of D-serine in the patients with AD were slightly (p = 0.078) lower than those of age- and gender-matched normal controls, while the L-serine levels in the patients were slightly (p = 0.083) higher.[54] Furthermore, Aβ and APP were both found to elevate D-serine and glutamate concentrations in cultured microglia and hippocampal neurons.[55−57] The dysregulation of serine metabolism is possibly implicated in the pathophysiology of AD.

In our study, the levels of threonine and valine were found to be increased in the brain of TASTPM mice. Threonine, an indirect precursor of valine, connects the glycine, serine and threonine metabolism pathway to valine, leucine and isoleucine biosynthesis. Interesting, an elevated level of glycine, valine, leucine, isoleucine, and other amino acids including aspartate and alanine were observed in specific brain regions of TgCRND8 mice via ^{1}H NMR-based metabonomics.[21] Similar to TASTPM mice, TgCRND8 is a transgenic strain that encodes a mutant form of the APP 695 and develops extracellular Aβ deposits as early as 2−3 months. Collectively, these data suggested that perturbations of amino acid metabolism play critical role in the pathogenesis of AD in Aβ mutant mouse models.

Zymosterol was decreased in the brain of TASTPM mice. Zymosterol, together with other sterols including cholesterol, are important metabolites in the pathway of steroid biosyn-

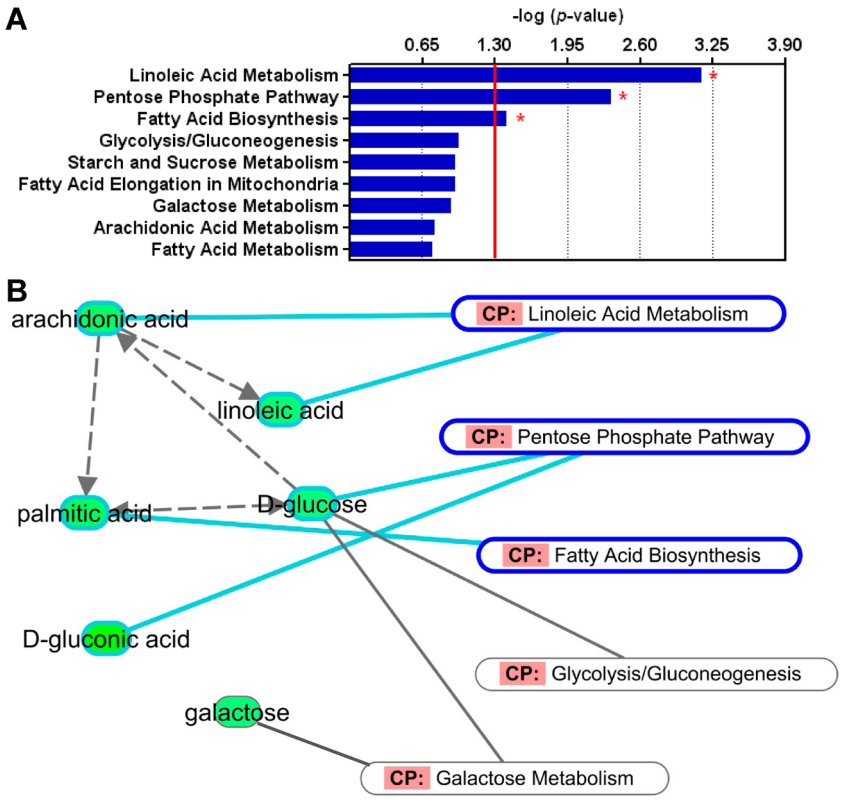

Figure 3. IPA of the significantly changed metabolites in the plasma samples of TASTPM mice when compared to wild-type mice. (A) Metabolic canonical pathways (CPs) significantly associated with the perturbed metabolites in TASTPM mice as indicated by the $-\log p > 1.30$ (equivalent to $p < 0.05$). The figure was regenerated on the basis of the data exported from the IPA analysis using GraphPad for high-resolution purpose. (B) IPA provided significant inter-relations among these perturbed metabolites (decreased as indicated in green) and the metabolic CPs (highlighted in blue box) in TASTPM mice. The marginally perturbed metabolic CPs were not highlighted in the blue box.

thesis. Zymosterol could be metabolized indirectly to cholesterol through multiple routes involving desmosterol. The decreased level of zymosterol in TASTPM mice is consistent with previous studies reporting the perturbation of steroid biosynthesis in AD. A clinical study found that desmosterol and desmosterol/cholesterol ratio were significantly decreased in plasma of AD patients compared with normal controls.[26] In a separate study, the plasma level of 5α-pregnan-3α-ol-20-one (3α,5α-THP) in AD demented subjects was found to be significantly lower compared with controls (25% decrease; $p = 0.004$).[58] In light of these studies and our observations, we further performed EIA on several endogenous steroids and determined that DHEA was relatively higher in both brain and plasma of TASTPM when compared to C57BL/6J mice. Interestingly, significantly higher DHEA levels in CSF[59] and increased total 7α-hydroxy-DHEA levels in serum[60] had been reported in AD patients. In addition, 17-OH-progesterone (precursor of androstenedione) and testosterone (metabolite of DHEA and 17-OH-progesterone) were significantly lower in brain and plasma of TASTPM mice. In addition, androstenedione (metabolite of DHEA and 17-OH-progesterone) was decreased significantly in brain and marginally in plasma of TASTPM mice, respectively. The change of 17-OH-progesterone levels may also contribute to the disease-related disturbances of DHEA production and metabolism, as they share a common precursor, which is 17-OH-pregnenolone. The observed changes in steroid levels in TASTPM mice and humans reflect a distorted secretion and/or alterations in metabolism of these hormones that in turn influence the symptomatology and progression of AD.[61,62]

Plasma

In plasma, all the marker metabolites were found to be decreased in TASTPM mice. It has been suggested that the two fatty acid biomarkers, linoleic acid and AA, are implicated in the pathogenesis of neurodegeneration, including AD.[63] Linoleic acid was reported to exert inhibitory effects on both Aβ42 cytotoxicity and cholesterol uptake in a Drosophila model, suggesting that it may be a potential candidate for the treatment of AD.[64] On the other hand, both linoleic acid and AA were observed to stimulate the assembly of tau protein and Aβ in brain neurons.[65] Neuropathological and epidemiological data suggest that neuroinflammation plays an important role in AD.[66] AA, a metabolite of linoleic acid, is the most important omega-6 fatty acid and an agonist of inflammatory pathways and stimulant of mucus secretion.[67] AA is typically attached at the central carbon of the glycerol backbone of phospholipids. The enzymes phospholipases A2 (PLA2), especially cytosolic PLA2 (cPLA2), releases AA preferentially from membrane phospholipids.[68] Previous studies have shown that aberrant action of this AA-selective PLA2 is associated with AD, and its activity can be stimulated by Aβ42.[69,70] Moreover, AA added to cells can directly initiate pathways that drive apoptosis in neurons.[71] In addition to directly contributing to the AD process, AA may be enzymatically metabolized to prostaglandins, thromboxanes and leukotrienes, to affect neuronal functions indirectly.[72] It has been suggested that the use of nonsteroidal anti-inflammatory drugs was associated with a

dx.doi.org/10.1021/pr300666p | J. Proteome Res. 2012, 11, 5903−5913

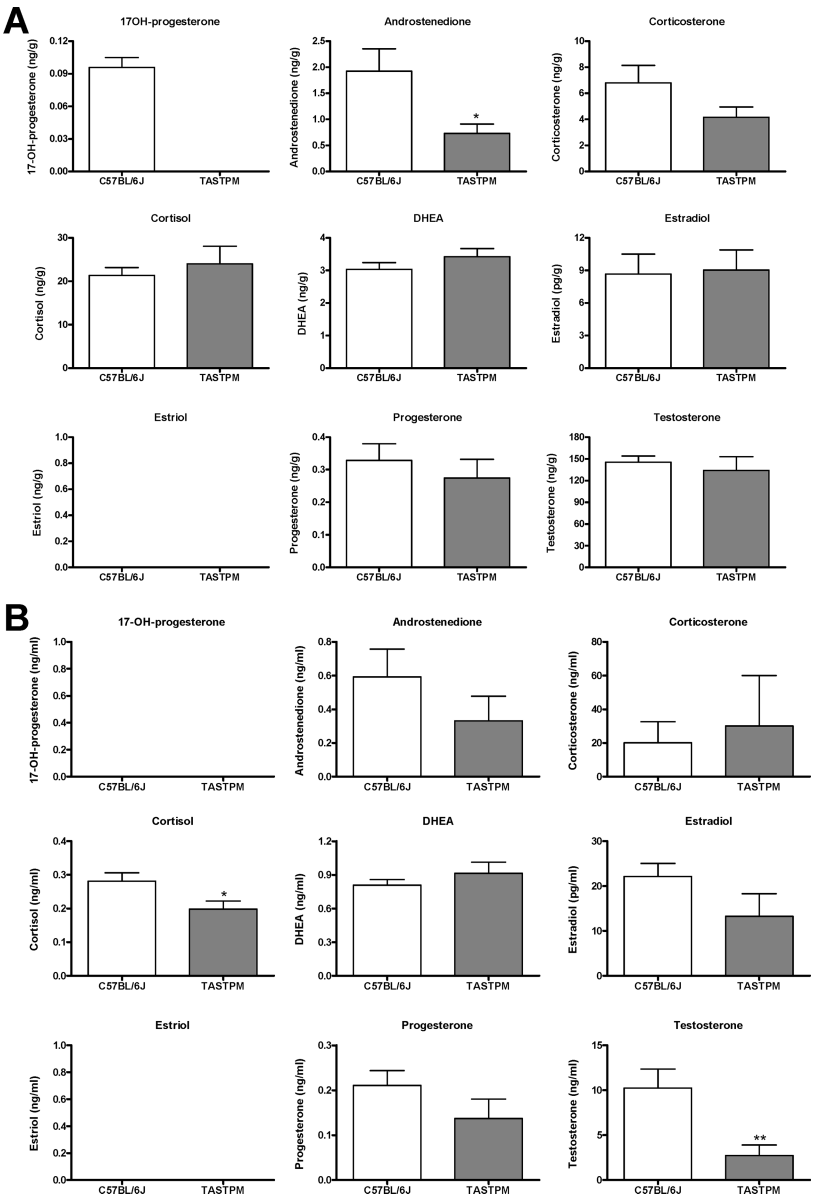

Figure 4. Steroid levels in whole brain (A) homogenate and (B) plasma of male TASTPM (n = 5) and C57BL/6J (n = 16) at the age of 50 weeks. Estriol was not detectable in brain samples, and both 17-OH-progesterone and estriol were not detectable in plasma samples. *p < 0.05; **p < 0.01; ***p < 0.001.

lower incidence of AD in human subjects.[73] In another study, three-five months treatment with triflusal, a compound with potent anti-inflammatory effects in the central nervous system, significantly reduced dense-cored plaque load and associated glial cell proliferation, proinflammatory cytokine levels and abnormal axonal curvature, and rescued cognitive deficits in an AD transgenic mouse model (Tg2576).[74] A direct imaging examination of radiolabeled AA in brains of live, non-anesthetized humans using positron emission tomography revealed increased AA metabolism in AD patients.[75] Interestingly, the reduced levels of linoleic acid and AA in our study also suggested upregulation of AA metabolism. Such elevated consumption of AA is consistent with evidence of inflammation and excitotoxicity in the post-mortem brain from AD patients.[76]

Our findings in plasma samples are highly consistent with a recently published metabonomics study in AD patients.[77] In this study, pathway analysis based on serum profiling revealed perturbed pentose phosphate pathway, fructose and mannose metabolism, galactose metabolism, fatty acid biosynthesis, etc. Pentose phosphate pathway was significantly perturbed when comparing progressive mild cognitive impairment (MCI) that developed AD with stable MCI groups. Interestingly, pentose phosphate pathway, galactose metabolism and fatty acid biosynthesis were also revealed by our IPA. It should be noted that the above-mentioned pathways are directly relevant to energy metabolism. In this respect, our findings on the lower levels of energy-related metabolites are consistent with previous studies showing that the energy metabolism was altered due to mitochondrial oxidative stress in AD.[25,78−82] Nevertheless, a recent study hypothesizes that the down-regulation of energy metabolism in AD could be a protective response of the neurons to the reduced level of nutrient and oxygen supply in the microenvironment.[83]

In summary, to the best of our knowledge, this is the first metabonomic study performed on both brain and plasma of the TASTPM mouse model. Our results confirmed a number of

dx.doi.org/10.1021/pr300666p | J. Proteome Res. 2012, 11, 5903−5913

metabolites were perturbed in both matrices of TASTPM mice. Without any a priori hypothesis regarding the involved biochemical pathways, GC−MS-based metabonomics identified a specific disease metabotype associated with AD as manifested in TASTPM mice. The disease metabotype is consistent with that of humans and reinforces the value of the transgenic AD mouse model in drug and biomarker development.

AUTHOR INFORMATION

Corresponding Author

*Tel: +65 65166137. Fax: +65 67791554. E-mail: phaccye@nus.edu.sg.

Notes

The authors declare no competing financial interest.

ACKNOWLEDGMENTS

We appreciate Ms. Lian Yee Yip for her assistance on chemometric data analysis and Dr. Boon-Seng Wong for his helpful discussion on the biological significances of our metabonomic findings. This project is supported by the Singapore Ministry of Education's (MOE) Academic Research Grant (R-148-000-135-112 to ECYC).

REFERENCES

(1) Braak, H.; Braak, E. Frequency of stages of Alzheimer-related lesions in different age categories. *Neurobiol. Aging* **1997**, *18* (4), 351−7.

(2) Pericak-Vance, M. A.; Bass, M. P.; Yamaoka, L. H.; Gaskell, P. C.; Scott, W. K.; Terwedow, H. A.; Menold, M. M.; Conneally, P. M.; Small, G. W.; Vance, J. M.; Saunders, A. M.; Roses, A. D.; Haines, J. L. Complete genomic screen in late-onset familial Alzheimer disease. Evidence for a new locus on chromosome 12. *JAMA, J. Am. Med. Assoc.* **1997**, *278* (15), 1237−41.

(3) Rogaev, E. I.; Sherrington, R.; Wu, C.; Levesque, G.; Liang, Y.; Rogaeva, E. A.; Ikeda, M.; Holman, K.; Lin, C.; Lukiw, W. J.; de Jong, P. J.; Fraser, P. E.; Rommens, J. M., St; George-Hyslop, P. Analysis of the 5′ sequence, genomic structure, and alternative splicing of the presenilin-1 gene (PSEN1) associated with early onset Alzheimer disease. *Genomics* **1997**, *40* (3), 415−24.

(4) Maes, O. C.; Xu, S.; Yu, B.; Chertkow, H. M.; Wang, E.; Schipper, H. M. Transcriptional profiling of Alzheimer blood mononuclear cells by microarray. *Neurobiol. Aging* **2007**, *28* (12), 1795−809.

(5) Unger, T.; Korade, Z.; Lazarov, O.; Terrano, D.; Schor, N. F.; Sisodia, S. S.; Mirnics, K. Transcriptome differences between the frontal cortex and hippocampus of wild-type and humanized presenilin-1 transgenic mice. *Am. J. Geriatr. Psychiatry* **2005**, *13* (12), 1041−51.

(6) Zhang, J.; Montine, T. J. Proteomic discovery of CSF biomarkers for Alzheimer's disease. *Ann. Neurol.* **2007**, *61* (5), 497,Author reply 497−8.

(7) Lovestone, S.; Guntert, A.; Hye, A.; Lynham, S.; Thambisetty, M.; Ward, M. Proteomics of Alzheimer's disease: understanding mechanisms and seeking biomarkers. *Expert Rev. Proteomics* **2007**, *4* (2), 227−38.

(8) Papassotiropoulos, A.; Fountoulakis, M.; Dunckley, T.; Stephan, D. A.; Reiman, E. M. Genetics, transcriptomics, and proteomics of Alzheimer's disease. *J. Clin. Psychiatry* **2006**, *67* (4), 652−70.

(9) Nicholson, J. K.; Lindon, J. C.; Holmes, E. "Metabonomics": understanding the metabolic responses of living systems to pathophysiological stimuli via multivariate statistical analysis of biological NMR spectroscopic data. *Xenobiotica* **1999**, *29* (11), 1181−9.

(10) Kaddurah-Daouk, R.; Kristal, B. S.; Weinshilboum, R. M. Metabolomics: A global biochemical approach to drug response and disease. *Annu. Rev. Pharmacol. Toxicol.* **2008**, *48*, 653−83.

(11) Bogdanov, M.; Matson, W. R.; Wang, L.; Matson, T.; Saunders-Pullman, R.; Bressman, S. S.; Flint Beal, M. Metabolomic profiling to develop blood biomarkers for Parkinson's disease. *Brain* **2008**, *131* (2), 389−96.

(12) Underwood, B. R.; Broadhurst, D.; Dunn, W. B.; Ellis, D. I.; Michell, A. W.; Vacher, C.; Mosedale, D. E.; Kell, D. B.; Barker, R. A.; Grainger, D. J.; Rubinsztein, D. C. Huntington disease patients and transgenic mice have similar pro-catabolic serum metabolite profiles. *Brain* **2006**, *129* (4), 877−86.

(13) Holmes, E.; Tsang, T. M.; Huang, J.T-H.; Markus Leweke, F.; Koethe, D.; Gerth, C. W.; Nolden, B. M.; Gross, S.; Schreiber, D.; Nicholson, J. K.; Bahn, S. Metabolic profiling of CSF: evidence that early intervention may impact on disease progression and outcome in schizophrenia. *PLoS Med.* **2006**, *3* (8), e327.

(14) Pears, M. R.; Cooper, J. D.; Mitchison, H. M.; Mortishire-Smith, R. J.; Pearce, D. A.; Griffin, J. L. High resolution ^{1}H NMR-based metabolomics indicates a neurotransmitter cycling deficit in cerebral tissue from a mouse model of Batten disease. *J. Biol. Chem.* **2005**, *280* (52), 42508−14.

(15) Dedeoglu, A.; Choi, J. K.; Cormier, K.; Kowall, N. W.; Jenkins, B. G. Magnetic resonance spectroscopic analysis of Alzheimer's disease mouse brain that express mutant human APP shows altered neurochemical profile. *Brain Res.* **2004**, *1012* (1−2), 60−5.

(16) von Kienlin, M.; Kunnecke, B.; Metzger, F.; Steiner, G.; Richards, J. G.; Ozmen, L.; Jacobsen, H.; Loetscher, H. Altered metabolic profile in the frontal cortex of PS2APP transgenic mice, monitored throughout their life span. *Neurobiol. Dis.* **2005**, *18* (1), 32−9.

(17) Marjanska, M.; Curran, G. L.; Wengenack, T. M.; Henry, P.-G.; Bliss, R. L.; Poduslo, J. F.; Jack, C. R., Jr.; Uğurbil, K.; Garwood, M. Monitoring disease progression in transgenic mouse models of Alzheimer's disease with proton magnetic resonance spectroscopy. *Proc. Natl. Acad. Sci. U. S. A.* **2005**, *102* (33), 11906−10.

(18) Jiang, N.; Yan, X.; Zhou, W.; Zhang, Q.; Chen, H.; Zhang, Y.; Zhang, X. NMR-based metabonomic investigations into the metabolic profile of the senescence-accelerated mouse. *J. Proteome Res.* **2008**, *7* (9), 3678−86.

(19) Tukiainen, T.; Tynkkynen, T.; Mäkinen, V. P.; Jylänki, P.; Kangas, A.; Hokkanen, J.; Vehtari, A.; Gröhn, O.; Hallikainen, M.; Soininen, H.; Kivipelto, M.; Groop, P. H.; Kaski, K.; Laatikainen, R.; Soininen, P.; Pirttilä, T.; Ala-Korpela, M. A multi-metabolite analysis of serum by (1)H NMR spectroscopy: Early systemic signs of Alzheimer's disease. *Biochem. Biophys. Res. Commun.* **2008**, *375* (3), 356−61.

(20) Greenberg, N.; Grassano, A.; Thambisetty, M.; Lovestone, S.; Legido-Quigley, C. A proposed metabolic strategy for monitoring disease progression in Alzheimer's disease. *Electrophoresis* **2009**, *30* (7), 1235−9.

(21) Salek, R. M.; Xia, J.; Innes, A.; Sweatman, B. C.; Adalbert, R.; Randle, S.; McGowan, E.; Emson, P. C.; Griffin, J. L. A metabolomic study of the CRND8 transgenic mouse model of Alzheimer's disease. *Neurochem. Int.* **2010**, *56* (8), 937−47.

(22) Li, N. J.; Liu, W. T.; Li, W.; Li, S. Q.; Chen, X. H.; Bi, K. S.; He, P. Plasma metabolic profiling of Alzheimer's disease by liquid chromatography/mass spectrometry. *Clin. Biochem.* **2010**, *43* (12), 992−7.

(23) Kaddurah-Daouk, R.; Rozen, S.; Matson, W.; Han, X.; Hulette, C. M.; Burke, J. R.; Doraiswamy, P. M.; Welsh-Bohmer, K. A. Metabolomic changes in autopsy-confirmed Alzheimer's disease. *Alzheimer's Dementia* **2011**, *7* (3), 309−17.

(24) Han, X.; Rozen, S.; Boyle, S. H.; Hellegers, C.; Cheng, H.; Burke, J. R.; Welsh-Bohmer, K. A.; Doraiswamy, P. M.; Kaddurah-Daouk, R. Metabolomics in early Alzheimer's disease: identification of altered plasma sphingolipidome using shotgun lipidomics. *PLoS One* **2011**, *6* (7), e21643.

(25) Trushina, E.; Nemutlu, E.; Zhang, S.; Christensen, T.; Camp, J.; Mesa, J.; Siddiqui, A.; Tamura, Y.; Sesaki, H.; Wengenack, T. M.; Dzeja, P. P.; Poduslo, J. F. Defects in mitochondrial dynamics and

metabolomic signatures of evolving energetic stress in mouse models of familial Alzheimer's disease. *PLoS One* **2012**, *7* (2), e32737.
(26) Sato, Y.; Suzuki, I.; Nakamura, T.; Bernier, F.; Aoshima, K.; Oda, Y. Identification of a new plasma biomarker of Alzheimer's disease using metabolomics technology. *J. Lipid Res.* **2012**, *53* (3), 567−76.
(27) Czech, C.; Berndt, P.; Busch, K.; Schmitz, O.; Wiemer, J.; Most, V.; Hampel, H.; Kastler, J.; Senn, H. Metabolite profiling of Alzheimer's disease cerebrospinal fluid. *PLoS One* **2012**, *7* (2), e31501.
(28) Shobab, L. A.; Hsiung, G. Y.; Feldman, H. H. Cholesterol in Alzheimer's disease. *Lancet Neurol.* **2005**, *4* (12), 841−52.
(29) Kivipelto, M.; Solomon, A. Cholesterol as a risk factor for Alzheimer's disease—epidemiological evidence. *Acta Neurol. Scand., Suppl.* **2006**, *185*, 50−7.
(30) Bornemann, K. D.; Wiederhold, K. H.; Pauli, C.; Ermini, F.; Stalder, M.; Schnell, L.; Sommer, B.; Jucker, M.; Staufenbiel, M. Abeta-induced inflammatory processes in microglia cells of APP23 transgenic mice. *Am. J. Pathol.* **2001**, *158* (1), 63−73.
(31) Boncristiano, S.; Calhoun, M. E.; Kelly, P. H.; Pfeifer, M.; Bondolfi, L.; Stalder, M.; Phinney, A. L.; Abramowski, D.; Sturchler-Pierrat, C.; Enz, A.; Sommer, B.; Staufenbiel, M.; Jucker, M. Cholinergic changes in the APP23 transgenic mouse model of cerebral amyloidosis. *J. Neurosci.* **2002**, *22* (8), 3234−43.
(32) van Dooren, T.; Dewachter, I.; Borghgraef, P.; van Leuven, F. Transgenic mouse models for APP processing and Alzheimer's disease: early and late defects. *Subcell. Biochem.* **2005**, *38*, 45−63.
(33) Pugh, P. L.; Richardson, J. C.; Bate, S. T.; Upton, N.; Sunter, D. Non-cognitive behaviours in an APP/PS1 transgenic model of Alzheimer's disease. *Behav. Brain Res.* **2007**, *178* (1), 18−28.
(34) Howlett, D. R.; Richardson, J. C.; Austin, A.; Parsons, A. A.; Bate, S. T.; Davies, D. C.; Gonzalez, M. I. Cognitive correlates of Abeta deposition in male and female mice bearing amyloid precursor protein and presenilin-1 mutant transgenes. *Brain Res.* **2004**, *1017* (1−2), 130−6.
(35) Howlett, D. R.; Bowler, K.; Soden, P. E.; Riddell, D.; Davis, J. B.; Richardson, J. C.; Burbidge, S. A.; Gonzalez, M. I.; Irving, E. A.; Lawman, A.; Miglio, G.; Dawson, E. L.; Howlett, E. R.; Hussain, I. Abeta deposition and related pathology in an APP x PS1 transgenic mouse model of Alzheimer's disease. *Histol. Histopathol.* **2008**, *23* (1), 67−76.
(36) Pardon, M. C.; Sarmad, S.; Rattray, I.; Bates, T. E.; Scullion, G. A.; Marsden, C. A.; Barrett, D. A.; Lowe, J.; Kendall, D. A. Repeated novel cage exposure-induced improvement of early Alzheimer's-like cognitive and amyloid changes in TASTPM mice is unrelated to changes in brain endocannabinoids levels. *Neurobiol. Aging* **2007**, *30* (7), 1099−113.
(37) Richardson, J. C.; Kendal, C. E.; Anderson, R.; Priest, F.; Gower, E.; Shoden, P.; Gray, R.; Topps, S.; Howlett, D. R.; Lavender, D.; Clarker, N. J.; Barnes, J. C.; Haworth, R.; Stewart, M. G.; Rupniak, H. T. R. Ultrastructural and behavioural changes precede amyloid deposition in a transgenic model of Alzheimer's disease. *Neuroscience* **2003**, *122* (1), 213−28.
(38) Sankaranarayanan, S. Genetically modified mice models for Alzheimer's disease. *Curr. Top. Med. Chem.* **2006**, *6* (6), 609−27.
(39) Chui, D. H.; Tanahashi, H.; Ozawa, K.; Ikeda, S.; Checler, F.; Ueda, O.; Suzuki, H.; Araki, W.; Inoue, H.; Shirotani, K.; Takahashi, K.; Gallyas, F.; Tabira, T. Transgenic mice with Alzheimer presenilin 1 mutations show accelerated neurodegeneration without amyloid plaque formation. *Nat. Med.* **1999**, *5* (5), 560−4.
(40) Holcomb, L.; Gordon, M. N.; McGowan, E.; Yu, X.; Benkovic, S.; Jantzen, P.; Wright, K.; Saad, I.; Mueller, R.; Morgan, D.; Sanders, S.; Zehr, C.; O'Campo, K.; Hardy, J.; Prada, C. M.; Eckman, C.; Younkin, S.; Hsiao, K.; Duff, K. Accelerated Alzheimer-type phenotype in transgenic mice carrying both mutant amyloid precursor protein and presenilin 1 transgenes. *Nat. Med.* **1998**, *4* (1), 97−100.
(41) Culbert, A. A.; Skaper, S. D.; Howlett, D. R.; Evans, N. A.; Facci, L.; Soden, P. E.; Seymour, Z. M.; Guillot, F.; Gaestel, M.; Richardson, J. C. MAPK-activated protein kinase 2 deficiency in microglia inhibits pro-inflammatory mediator release and resultant neurotoxicity. Relevance to neuroinflammation in a transgenic mouse model of Alzheimer disease. *J. Biol. Chem.* **2006**, *281* (33), 23658−67.
(42) A, J.; Trygg, J.; Gullberg, J.; Johansson, A. I.; Jonsson, P.; Antti, H.; Marklund, S. L.; Moritz, T. Extraction and GC/MS analysis of the human blood plasma metabolome. *Anal. Chem.* **2005**, *77* (24), 8086−94.
(43) Denkert, C.; Budczies, J.; Kind, T.; Weichert, W.; Tablack, P.; Sehouli, J.; Silvia, N.; Könsgen, D.; Dietel, M.; Fiehn, O. Mass spectrometry-based metabolic profiling reveals different metabolite patterns in invasive ovarian carcinomas and ovarian borderline tumors. *Cancer Res.* **2006**, *66* (22), 10795−804.
(44) Liere, P.; Akwa, Y.; Weill-Engerer, S.; Eychenne, B.; Pianos, A.; Robel, P.; Sjovall, J.; Schumacher, M.; Baulieu, E. E. Validation of an analytical procedure to measure trace amounts of neurosteroids in brain tissue by gas chromatography-mass spectrometry. *J. Chromatogr., B: Biomed. Sci. Appl.* **2000**, *739* (2), 301−12.
(45) Fekkes, D.; van der Cammen, T. J. M.; van Loon, C. P. M.; Verschoor, C.; van Harskamp, F.; de Koning, I.; Schudel, W. J.; Pepplinkhuizen, L. Abnormal amino acid metabolism in patients with early stage Alzheimer dementia. *J. Neural Transm.* **1998**, *105* (2−3), 287−94.
(46) Haughey, N. J.; Bandaru, V. V.; Bae, M.; Mattson, M. P. Roles for dysfunctional sphingolipid metabolism in Alzheimer's disease neuropathogenesis. *Biochim. Biophys. Acta* **2010**, *1801* (8), 878−86.
(47) Prasad, M. R.; Lovell, M. A.; Yatin, M.; Dhillon, H.; Markesbery, W. R. Regional membrane phospholipid alterations in Alzheimer's disease. *Neurochem. Res.* **1998**, *23* (1), 81−8.
(48) Han, X.; M Holtzman, D.; McKeel, D. W., Jr.; Kelley, J.; Morris, J. C. Substantial sulfatide deficiency and ceramide elevation in very early Alzheimer's disease: potential role in disease pathogenesis. *J. Neurochem.* **2002**, *82* (4), 809−18.
(49) He, X.; Huang, Y.; Li, B.; Gong, G. X.; Schuchman, E. H. Deregulation of sphingolipid metabolism in Alzheimer's disease. *Neurobiol. Aging* **2010**, *31* (3), 398−408.
(50) Rodriguez-Crespo, I. D-Amino acids in the brain: pyridoxal phosphate-dependent amino acid racemases and the physiology of D-serine. *FEBS J.* **2008**, *275* (14), 3513.
(51) Suh, Y. H.; Checler, F. Amyloid precursor protein, presenilins, and alpha-synuclein: molecular pathogenesis and pharmacological applications in Alzheimer's disease. *Pharmacol. Rev.* **2002**, *54* (3), 469−525.
(52) Wolosker, H.; Dumin, E.; Balan, L.; Foltyn, V. N. D-Amino acids in the brain: D-serine in neurotransmission and neurodegeneration. *FEBS J.* **2008**, *275* (14), 3514−26.
(53) Mothet, J. P.; Parent, A. T.; Wolosker, H.; Brady, R. O., Jr.; Linden, D. J.; Ferris, C. D.; Rogawski, M. A.; Snyder, S. H. D-serine is an endogenous ligand for the glycine site of the *N*-methyl-D-aspartate receptor. *Proc. Natl. Acad. Sci. U. S. A.* **2000**, *97* (9), 4926−31.
(54) Hashimoto, K.; Fukushima, T.; Shimizu, E.; Okada, S.; Komatsu, N.; Okamura, N.; Koike, K.; Koizumi, H.; Kumakiri, C.; Imai, K.; Iyo, M. Possible role of D-serine in the pathophysiology of Alzheimer's disease. Prog. *Neuropsychopharmacol. Biol. Psychiatry* **2004**, *28* (2), 385−8.
(55) Brito-Moreira, J.; C. Paula-Lima, A.; R. Bomfim, T.; F. Oliveira, F.; J. Sepulveda, F.; G. De Mello, F.; G. Aguayo, L.; Panizzutti, R.; T. Ferreira, S. Abeta oligomers induce glutamate release from hippocampal neurons. *Curr. Alzheimer Res.* **2011**, *8* (5), 552−62.
(56) Wu, S. Z.; Basile, A. S.; Barger, S. W. Induction of serine racemase expression and D-serine release from microglia by secreted amyloid precursor protein (sAPP). *Curr. Alzheimer Res.* **2007**, *4* (3), 243−51.
(57) Wu, S. Z.; Bodles, A. M.; Porter, M. M.; T Griffin, W. S.; Basile, A. S.; Barger, S. W. Induction of serine racemase expression and D-serine release from microglia by amyloid beta-peptide. *J. Neuroinflammation* **2004**, DOI: 10.1186/1742-2094-1-2.
(58) Smith, C. D.; Wekstein, D. R.; Markesbery, W. R.; Frye, C. A. 3alpha,5alpha-THP: a potential plasma neurosteroid biomarker in Alzheimer's disease and perhaps non-Alzheimer's dementia. *Psychopharmacology* **2006**, *186* (3), 481−5.

(59) Kim, S. B.; Kim, M.; Kwak, Y. T.; Hampl, R.; Jo, D. H.; Morfin, R. Neurosteroids: Cerebrospinal fluid levels for Alzheimer's disease and vascular dementia diagnostics. *J. Clin. Endocrinol. Metab.* **2003**, *88* (11), 5199−206.
(60) Attal-Khemis, S.; Dalmeyda, V.; Michot, J. L.; Roudier, M.; Morfin, R. Increased total 7 alpha-hydroxy-dehydroepiandrosterone in serum of patients with Alzheimer's disease. *J. Gerontol., Ser. A* **1998**, *53* (2), B125−32.
(61) Rasmuson, S.; Nasman, B.; Carlstrom, K.; Olsson, T. Increased levels of adrenocortical and gonadal hormones in mild to moderate Alzheimer's disease. *Dementia Geriatr. Cognit. Disord.* **2002**, *13* (2), 74−9.
(62) Baulieu, E. E.; Robel, P.; Schumacher, M. Neurosteroids: beginning of the story. *Int. Rev. Neurobiol.* **2001**, *46*, 1−32.
(63) Montine, T. J.; Morrow, J. D. Fatty acid oxidation in the pathogenesis of Alzheimer's disease. *Am. J. Pathol.* **2005**, *166* (5), 1283−9.
(64) Lee, M. J.; Park, S. H.; Han, J. H.; Hong, Y. K.; Hwang, S.; Lee, S.; Kim, D.; Han, S. Y.; Kim, E. S.; Cho, K. S. The effects of hempseed meal intake and linoleic acid on Drosophila models of neurodegenerative diseases and hypercholesterolemia. *Mol. Cells* **2011**, *31* (4), 337−42.
(65) Wilson, D. M.; Binder, L. I. Free fatty acids stimulate the polymerization of tau and amyloid beta peptides. In vitro evidence for a common effector of pathogenesis in Alzheimer's disease. *Am. J. Pathol.* **1997**, *150* (6), 2181−95.
(66) Wyss-Coray, T. Inflammation in Alzheimer disease: driving force, bystander or beneficial response? *Nat. Med.* **2006**, *12* (9), 1005−15.
(67) Srinivasan, B. D.; Kulkarni, P. S. Inhibitors of the arachidonic acid cascade in the management of ocular inflammation. *Prog. Clin. Biol. Res.* **1989**, *312*, 229−49.
(68) Burke, J. E.; Dennis, E. A. Phospholipase A2 structure/function, mechanism, and signaling. *J. Lipid Res.* **2009**, *50* (Suppl), S237−42.
(69) Stephenson, D.; Rash, K.; Smalstig, B.; Roberts, E.; Johnstone, E.; Sharp, J.; Panetta, J.; Little, S.; Kramer, R.; Clemens, J. Cytosolic phospholipase A2 is induced in reactive glia following different forms of neurodegeneration. *Glia* **1999**, *27* (2), 110−28.
(70) Sanchez-Mejia, R. O.; Newman, J. W.; Toh, S.; Yu, G. Q.; Zhou, Y.; Halabisky, B.; Cissé, M.; Scearce-Levie, K.; Cheng, I. H.; Gan, L.; Palop, J. J.; Bonventre, J. V.; Mucke, L. Phospholipase A2 reduction ameliorates cognitive deficits in a mouse model of Alzheimer's disease. *Nat. Neurosci.* **2008**, *11* (11), 1311−8.
(71) Lipton, P. Ischemic cell death in brain neurons. *Phys. Rev.* **1999**, *79* (4), 1431−568.
(72) Sanchez-Mejia, R. O.; Mucke, L. Phospholipase A2 and arachidonic acid in Alzheimer's disease. *Biochim. Biophys. Acta* **2010**, *1801* (8), 784−90.
(73) Côté, S.; Carmichael, P. H.; Verreault, R.; Lindsay, J.; Lefebvre, J.; Laurin, D. Nonsteroidal anti-inflammatory drug use and the risk of cognitive impairment and Alzheimer's disease. *Alzheimer's Dementia* **2012**, *8* (3), 219−26.
(74) Coma, M.; Serenó, L.; Da Rocha-Souto, B.; Scotton, T. C.; España, J.; Sánchez, M. B.; Rodríguez, M.; Agulló, J.; Guardia-Laguarta, C.; Garcia-Alloza, M.; Borrelli, L. A.; Clarimón, J.; Lleó, A.; Bacskai, B. J.; Saura, C. A.; Hyman, B. T.; Gómez-Isla, T. Triflusal reduces dense-core plaque load, associated axonal alterations and inflammatory changes, and rescues cognition in a transgenic mouse model of Alzheimer's disease. *Neurobiol. Dis.* **2010**, *38* (3), 482−91.
(75) Esposito, G.; Giovacchini, G.; Liow, J. S.; Bhattacharjee, A. K.; Greenstein, D.; Schapiro, M.; Hallett, M.; Herscovitch, P.; Eckelman, W. C.; Carson, R. E.; Rapoport, S. I. Imaging neuroinflammation in Alzheimer disease with radiolabeled arachidonic acid and PET. *J. Nucl. Med.* **2008**, *49* (9), 1414−21.
(76) McGeer, P. L.; McGeer, E. G. NSAIDs and Alzheimer disease: epidemiological, animal model and clinical studies. *Neurobiol. Aging* **2007**, *28* (5), 639−47.
(77) Orešič, M.; Hyötyläinen, T.; Herukka, S.-K.; Sysi-Aho, M.; Mattila, I.; Seppänan-Laakso, T.; Julkunen, V.; Gopalacharyulu, P. V.; Hallikainen, M.; Koikkalainen, J.; Kivipelto, M.; Helisalmi, S.; Lötjönen, J.; Soininen, H. Metabolome in progression to Alzheimer's disease. *Transl. Psychiatry* **2011**, *1*, e57.
(78) Ferrer, I. Altered mitochondria, energy metabolism, voltage-dependent anion channel, and lipid rafts converge to exhaust neurons in Alzheimer's disease. *J. Bioenerg. Biomembr.* **2009**, *41* (5), 425−31.
(79) Ogawa, M.; Fukuyama, H.; Ouchi, Y.; Yamauchi, H.; Kimura, J. Altered energy metabolism in Alzheimer's disease. *J. Neurol. Sci.* **1996**, *139* (1), 78−82.
(80) Atamna, H.; Frey, W. H., 2nd. Mechanisms of mitochondrial dysfunction and energy deficiency in Alzheimer's disease. *Mitochondrion* **2007**, *7* (5), 297−310.
(81) Blass, J. P.; Sheu, R. K.; Gibson, G. E. Inherent abnormalities in energy metabolism in Alzheimer disease. Interaction with cerebrovascular compromise. *Ann. N. Y. Acad. Sci.* **2000**, *903*, 204−21.
(82) Beal, M. F. Oxidative damage as an early marker of Alzheimer's disease and mild cognitive impairment. *Neurobiol. Aging* **2005**, *26* (5), 585−6.
(83) Sun, J.; Feng, X.; Liang, D.; Duan, Y.; Lei, H. Down-regulation of energy metabolism in Alzheimer's disease is a protective response of neurons to the microenvironment. *J. Alzheimer's Dis.* **2012**, *28* (2), 389−402.